Journal of Applied Physics ARTICLE scitation.org/journal/jap

Absolute photoluminescence intensity in thin film solar cells

Cite as: J. Appl. Phys. **125**, 053103 (2019); doi: 10.1063/1.5064798
Submitted: 8 October 2018 · Accepted: 14 January 2019 ·
Published Online: 6 February 2019

View Online Export Citation CrossMark

C. H. Swartz,[1,a)] S. Paul,[2] L. M. Mansfield,[3] and M. W. Holtz[2]

AFFILIATIONS

[1]Materials Science, Engineering, and Commercialization Program, Texas State University, San Marcos, Texas 78666, USA
[2]Department of Physics, Texas State University, San Marcos, Texas 78666, USA
[3]National Renewable Energy Laboratory, Golden, Colorado 80401, USA

[a)]Author to whom correspondence should be addressed: craig.swartz@txstate.edu

ABSTRACT

A calculation is presented for the direct conversion of a measured luminescence signal to the implied open circuit voltage. The effects of re-absorption, spectral dependence, and interference with front and back interfaces are all included, so long as the optical properties of the structure are known. The method is validated through a comparison of the terminal open-circuit voltage with the photoluminescence intensity of Cu(In,Ga)Se_2 solar cells, each as a function of illumination intensity.

I. INTRODUCTION

Luminescence imaging is a measurement technique used for development and rapid assessment of photovoltaic devices.[1] Since the luminescence intensity has an exponential dependence on the quasi-Fermi level splitting between electrons and holes, ΔE_F in Fig. 1(a), the implied open circuit voltage can be probed, even before the fabrication of an electrical contact structure.

For a luminescence signal to take on a quantitative meaning, its relationship with the implied open circuit voltage must be calibrated. This can be done by determining photoluminescence (PL) or electroluminescence (EL) signals at several excitation (intensity) levels and solving for ΔE_F within a multiple diode circuit model.[2] Alternatively, the effective carrier lifetime may be independently estimated with some other measurements such as photoconductance and the corresponding ΔE_F determined.[3] However, uncertainty remains about the level of detail needed in a circuit model to give reliable results.[4,5] Any such circuit analysis will also depend upon approximations such as excitation-independent photocarrier lifetimes. Scaling factors relating a measured PL signal to ΔE_F are desirable for contactless characterization of solar cells and potentially other optoelectronic devices.

A number of authors have related ΔE_F to absolute measurements of PL magnitude (in photons $m^{-2}\,s^{-1}$) by way of

$$N(E)dE = \frac{a(E)\ \Omega}{4\pi^3\hbar^3c^2}\frac{E^2}{\exp\left(\frac{(E-\Delta E_F)}{k_BT}\right)-1}\ dE, \tag{1}$$

which is the "Lasher-Stern-Wurfel" (LSW) formula.[6–9] This generalized form of both Planck's Law and the van Roosbroeck-Shockley (VRS) relation applies to band-to-band PL in a material with a non-equilibrium density of excited electrons and holes which have each reached a quasi-equilibrium within the conduction and valence bands, respectively. In Eq. (1), Ω is the solid angle through which detected photons of energy $E = \hbar\omega$ pass. The optical absorption coefficient $\alpha(E)$ of the material is contained within the absorptivity

$$a(E) = 1 - \exp\left[-\alpha(E)d\right], \tag{2}$$

where d is the thickness of the radiating layer. The other symbols in Eq. (1) have their usual meanings.

The spectrally resolved PL is related to $\alpha(E)$ by the LSW formula. Figure 1(b) shows the energy dependence for $\alpha(E)$[10] and the corresponding N(E) from Eq. (1). By restricting the analysis to PL photon energies somewhat above the bandgap (E_G), the quantities $\alpha(E)d$ and $\exp\left[(E-\Delta E_F)/k_BT\right]$ are both $\gg 1$, the absorptivity becomes 1, and the energy-dependent PL

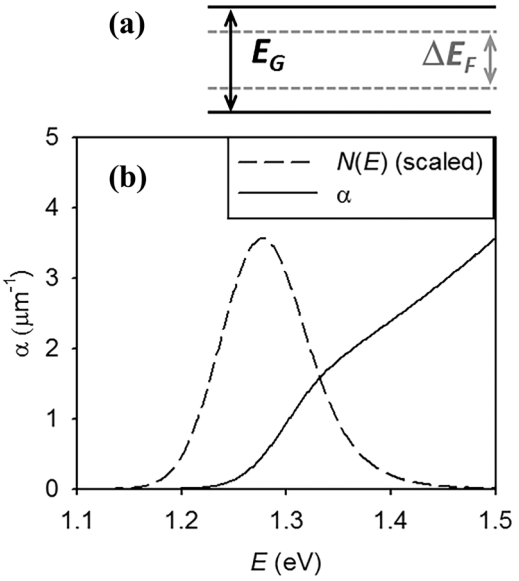

FIG. 1. (a) An illustration of electron and hole Fermi levels separated and within the gap of a semiconductor. (b) The absorption coefficient of $CuIn_{1-0.5}Ga_{0.5}Se_2$ (E_G = 1.3 eV) taken from Ref. 10, with the resulting normalized PL intensity calculated from Eq. (1).

expression for N(E) in Eq. (1) may be rewritten as

$$\ln\left(\frac{dN(E)}{E^2}\right) \approx \ln\left(\frac{\Omega dE}{4\pi^3\hbar^3c^2}\right) - \frac{(E-\Delta E_F)}{k_BT}, \tag{3}$$

which gives ΔE_F as an offset to the PL magnitude versus energy relationship without reference to thickness or $a(E)$. However, ambiguities and unrealistic results often follow from the subjective choice of high energy range for $a(E)$. Possibly, this is because solving for ΔE_F involves extrapolating Eq. (3) to the $E \to 0$ limit, amplifying any variations from the chosen fit range or from non-uniform composition. Authors have attempted to instead fit the entire PL spectrum, although this relies on adopting an uncertain absorption tail model at low energies and is particularly problematic in multilayer structures.[7,8]

One alternative is to use the full, integrated PL intensity. Although this would invalidate the simplifying assumption of $a(E) = 1$, the overall intensity should be fairly insensitive to uncertainties resulting from extrapolating the dependence in Eq. (3) to $E \to 0$ and from the precise details of low energy tailing.

Since the total luminescence efficiency of a solar cell is directly related to its power generation efficiency,[11,12] a number of calculations have already been put forward for the absolute emission rate of photons from a layered structure. Re-absorption and multiple front and back interface reflections should be considered[13,14] as well as the angular and spectral dependence of the reflection and absorption.[15] While interference is typically ignored with the use of ray optics, it can become significant with thin films, particularly those with a composition grading that changes over length scales less than the order of the wavelength.

Surprisingly, there does not appear to be any reported calculation relating ΔE_F within layered structures to external emission rates, which quantitatively accounts for interference and re-absorption. One attempt was made to include all such effects, by finding the Poynting vector using the fluctuation-dissipation theorem.[16] However, the resulting Poynting vector was not proportional to $a(E)$ for thin layers, in contradiction to the LSW formula. Also, the fluctuation-dissipation theorem applies only in thermal equilibrium conditions, not simply to steady state conditions where thermal equilibrium has not been established.[17]

Another calculation, taking into account interference in a graded-gap $CuIn_{1-x}Ga_xSe_2$ (CIGS) material stack,[18] combined the LSW formula with an expression ultimately due to Lukosz.[19,20] This approach gave the power of optical emission into an infinite medium (such as air) from an ensemble of radiating dipoles embedded in a slab of known dielectric properties, without considering re-absorption. However, inspection reveals that in the homogeneous case, when the slab has the same index as the infinite medium, this expression yields an unphysical result which continues to depend on the thickness of the slab.[20] A reformulation of the Lukosz expression by Broeck had similar problems in the homogeneous case, with the s-polarized power increasing as the surrounding medium's index of refraction increased.[21] Other closed-form expressions which have been reported for dipole radiation through interfaces apply to a dipole embedded in a semi-infinite medium, rather than within a film.[22,23] A recently reported calculation included interference and re-absorption in relating radiative recombination rates, at a given depth and energy, to external emission rates,[24] although the result was not in the closed-form and was computationally intensive.[25]

This work presents a method of calculating the external emission of luminescence from an excited semiconductor within a layered structure of known optical properties. Sipe's dyadic Green's functions[26] are used to find a closed-form expression for the impact of the structure on the external emission from a randomly oriented dipole radiation source at a given energy and location. The absolute emission at an energy E resulting from a value of ΔE_F at a given location is taken from the LSW formula.

II. THEORY

We wish to find the electric field in a medium with index of refraction n_1, caused by a single dipole $\vec{P}_0$ depicted in Fig. 2 at position $x = y = 0$, $z = z_0$ and oscillating with frequency

$$\omega = k_0c = \frac{E}{\hbar} \tag{4}$$

inside of a slab of thickness d and (complex valued) index of refraction n_3. The polarization due to the dipole is

$$\vec{P} = \vec{P}_0\delta(x)\delta(y)\delta(z - z_0), \tag{5}$$

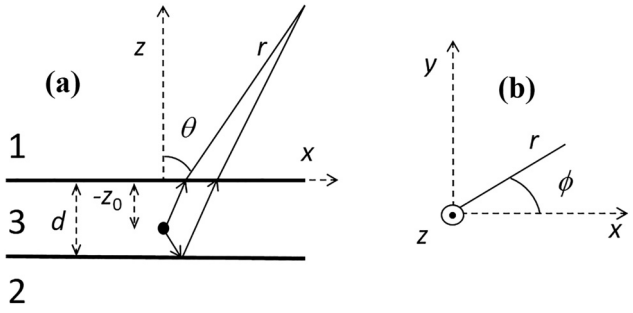

FIG. 2. Geometry of a dipole embedded in a slab (3) of known dielectric properties, between two interfaces, which emits energy into a surrounding medium (1). (a) The *xz* plane is shown. (b) The *xy* plane, which is the surface of the slab (3), is shown from above.

where the time dependence has been suppressed. While the electric field has not been explicitly given in the literature, the field for a thin sheet (at $z = z_0$) of periodic polarization with a sinusoidally varying density has been solved.[26] Therefore, we expand the delta functions $\delta(x)\delta(y)$ in the polarization into a sinusoidal sheet representation

$$\vec{P} = \vec{P}_0\delta(z - z_0)\,(2\pi)^{-2}\int\int_{-\infty}^{+\infty}\exp\,(ik_x x + ik_y\,y)\mathrm{d}k_x\mathrm{d}k_y$$
$$= \vec{P}_0\delta(z - z_0)\,(2\pi)^{-2}\int_0^{2\pi}\int_0^{\infty}\exp\,(ik\cos\varphi x + ik\sin\varphi\,y)\,k\mathrm{d}k\mathrm{d}\varphi. \tag{6}$$

For a given sheet of polarization

$$\vec{P}_{sh} = \vec{P}_0\,k\mathrm{d}k\mathrm{d}\varphi\,(2\pi)^{-2}\exp\,(ik\cos\varphi x + ik\sin\varphi\,y)\delta(z - z_0), \tag{7}$$

the electric field was found to be[26]

$$\vec{E}_s = A_s(k)\mathrm{d}k\mathrm{d}\varphi\,\gamma_z\begin{pmatrix}\gamma_\varphi\sin^2\varphi & -\gamma_\varphi\sin(2\varphi)/2 & 0\\ -\gamma_\varphi\sin(2\varphi)/2 & \gamma_\varphi\cos^2\varphi & 0\\ 0 & 0 & 0\end{pmatrix}\vec{P}_0$$
$$= \overleftrightarrow{G}_s(k,\ \varphi)\ \vec{P}_0 \tag{8}$$

for s-polarized radiation, where

$$A_s(k) = \frac{ik\,k_0^2\,t_{31s}(k)(\beta_s + 1)}{2\pi\,\gamma_0\,w_3\mu_s} \tag{9}$$

and

$$\begin{aligned}\gamma_z &= \exp\,(iw_1 z),\\ \gamma_0 &= \exp\,(iw_3 z_0),\\ \gamma_d &= \exp\,(i2w_3 d),\\ \gamma_\varphi &= \exp(ikx\cos\varphi),\\ \beta_s &= \gamma_0^2\,\gamma_d\,r_{32s}(k),\\ \mu_s &= \gamma_d\,r_{31s}(k)\,r_{32s}(k) - 1\,.\end{aligned} \tag{10}$$

The in-plane wavenumber has magnitude k and azimuthal direction φ, and it does not change from layer to layer. The z-component wavenumbers are $w_1^2 = n_1k_0^2 - k^2$ and $w_3^2 = n_3k_0^2 - k^2$. The reflection and transmission coefficients from the slab to the observer's medium are r_{31} and t_{31}, and the back or bottom interface reflection coefficient is r_{32}. The reflection and transmission coefficients are labeled with s or p for the differing values they will take from the Fresnel equations for incident s- and p-polarized light, at a transmitted angle of

$$\sin\theta_t = \frac{k}{k_0 n_1} \tag{11}$$

from Snell's law.

The classic Fresnel formulas for a single interface are

$$r_{ijs} = \frac{w_i - w_j}{w_i + w_j},\ t_{ijs} = \frac{2w_i}{w_i + w_j},\ r_{ijp} = \frac{w_i n_j^2 - w_j n_i^2}{w_i n_j^2 + w_j n_i^2},\ t_{ijp} = \frac{2n_i n_j}{w_i n_j^2 + w_j n_i^2}, \tag{12}$$

but the reflection and transmission coefficients are not limited to these since the back interface may be reflecting (e.g., a metallic contact) and the front interface in particular may have multiple layers. Multi-layered interfaces may be combined into a single pair of effective reflection and transmission coefficients using a coherent matrix formalism.[27] Since dipole moments of x and y orientation are fully included, we have without loss of generality evaluated the fields only for an observer in the xz plane at a distance $r^2 = x^2 + z^2$ and polar angle θ.

We integrate each sheet over $\mathrm{d}k\mathrm{d}\varphi$ to obtain the resultant electric field from a single oscillating dipole. The magnitude of the Poynting vector, and hence power per area, is then found from

$$|\vec{S}| = \frac{c}{8\pi}|\vec{E}|^2. \tag{13}$$

However, note that the field cannot be squared until the integral over $\mathrm{d}k\mathrm{d}\varphi$ is carried out; for the various planar wave components to combine to form a polarization delta function, they must be oscillating in-phase and thus able to mutually interfere. Only after the electric field due to a delta function source is found can they be viewed as separate sources emitting incoherently, with additive $\vec{S}$ values.

Taking the center element of $\overleftrightarrow{G}_s$,

$$\int\int G_{s22}(k,\ \varphi)\mathrm{d}\varphi\mathrm{d}k = \int_0^{\infty}A_s(k)\gamma_z\int_0^{2\pi}\exp\,(ikx\cos\varphi)\cos^2\varphi\mathrm{d}\varphi\mathrm{d}k, \tag{14}$$

the φ integral may be solved using Bessel functions. At this point, we take the fields at a macroscopically distant detector, so that the observer distance $r^2 = x^2 + z^2$ is many wavelengths from the layered structure. This allows us to use the asymptotic form of the Bessel functions[22] so that the right-hand

side of Eq. (14) may be written as

$$= \int A_s(k)\gamma_z \pi[J_0(kx) - J_2(kx)]\ \mathrm{d}k \rightarrow \int A_s(k)\gamma_z \sqrt{\frac{2\pi}{kx}}\cos\left(kx - \frac{\pi}{4}\right)\ \mathrm{d}k. \tag{15}$$

The remaining elements of $\overleftrightarrow{G}_s$ become zero after φ integration.

The macroscopic observer distance allows us to evaluate the integral over $\mathrm{d}k$ using the stationary phase method.[28] Defining

$$\begin{aligned} g_1 &= w_1 z + kx - \frac{\pi}{4}, \\ g_2 &= w_1 z - kx + \frac{\pi}{4}, \end{aligned} \tag{16}$$

we have

$$\int A_s(k)\gamma_z \sqrt{\frac{2\pi}{kx}}\cos\left(kx - \frac{\pi}{4}\right)\mathrm{d}k = \int A_s(k)\sqrt{\frac{\pi}{2kx}}[\exp(ig_1) + \exp(ig_2)]\ \mathrm{d}k. \tag{17}$$

At macroscopic distances, the products kx and $w_1 z$ are very large. Therefore, $A_s(k)$ is slowly varying, and the dominant range of the integral is in the neighborhood of the stationary points of the phases g_i. Recalling that w_1 is a function of k, the phase

$$g_1(k) = z\sqrt{k_0^2 n_1^2 - k^2} + kx - \frac{\pi}{4} \tag{18}$$

has a stationary point at $g_1'(k_c) = 0$, which is solved by

$$k_c = \frac{k_0 n_1 x}{r} = k_0 n_1 \sin\theta. \tag{19}$$

Note from Eq. (11) that this value of k_c corresponds to $\theta_t = \theta$ or propagation in the direction of the observer angle. Since the phase g_2 has no real positive stationary point, the integral is then solved by[28]

$$\int A_s(k)\sqrt{\frac{\pi}{2kx}}[\exp(ig_1)]\mathrm{d}k \cong A_s(k_c)\sqrt{\frac{\pi}{2k_c x}}\sqrt{\frac{2i\pi}{g''_1(k_c)}} \tag{20}$$

for a total electric field of

$$\vec{E}_{stot} = \frac{\pi A_s(k_c)}{\sqrt{-ik_{st}xg''_1(k_c)}}\begin{pmatrix} 0 & 0 & 0 \\ 0 & 1 & 0 \\ 0 & 0 & 0 \end{pmatrix}\vec{P}_0 = \overleftrightarrow{G}_{stot}\vec{P}_0. \tag{21}$$

For p-polarized light, the field for a sheet of oscillating polarization is[26]

$$\begin{aligned} \vec{E}_p &= A_p(k)\mathrm{d}k\mathrm{d}\varphi\gamma_z \\ &\times \begin{pmatrix} -w_1 w_3(\beta_p - 1)\gamma_\varphi \cos^2\varphi & 0 & -kw_1(\beta_p + 1)\gamma_\varphi \cos\varphi \\ 0 & 0 & 0 \\ kw_3(\beta_p - 1)\gamma_\varphi \cos\varphi & 0 & k^2(\beta_p + 1)\gamma_\varphi \end{pmatrix}\vec{P}_0 \\ &= \overleftrightarrow{G}_p(k, \varphi)\vec{P}_0, \end{aligned} \tag{22}$$

where

$$A_p(k) = \frac{ikt_{31p}(k)}{2\pi\gamma_0 n_1 n_3 w_3 \mu_p}. \tag{23}$$

For brevity, the elements that will integrate to zero over φ have already been dropped.

The integral over φ is carried out as before, this time leaving more than one nonzero element

$$\begin{aligned} &\iint \overleftrightarrow{G}_p(k,\ \varphi)\ \mathrm{d}\varphi\mathrm{d}k\ \vec{P}_0 \\ &= \int A_p(k)\gamma_z \begin{pmatrix} -w_1 w_3(\beta_p - 1) & 0 & ikw_1(\beta_p + 1) \\ 0 & 0 & 0 \\ -ikw_3(\beta_p - 1) & 0 & ik^2(\beta_p + 1) \end{pmatrix} \\ &\times \sqrt{\frac{2\pi}{kx}}\cos\left(kx - \frac{\pi}{4}\right)\mathrm{d}k\ \vec{P}_0. \end{aligned} \tag{24}$$

For each element, the same phases g and stationary point k_c still occur, for a total electric field of

$$\begin{aligned} \vec{E}_{ptot} &= \frac{\pi A_p(k_c)}{\sqrt{-ik_c x g''_1(k_c)}} \\ &\times \begin{pmatrix} -w_{1c}w_{3c}(\beta_{pc} - 1) & 0 & ik_c w_{1c}(\beta_{pc} + 1) \\ 0 & 0 & 0 \\ -ik_c w_{3c}(\beta_{pc} - 1) & 0 & ik_c^2(\beta_{pc} + 1) \end{pmatrix}\vec{P}_0, \\ &= \overleftrightarrow{G}_{ptot}\vec{P}_0, \end{aligned} \tag{25}$$

where the subscript c indicates that k_c is substituted for k within that term. This solves for the electric field due to both polarizations, providing the dyadic Green's function relating a dipole moment to the electric field at a macroscopically distant observer

$$\vec{E}_{tot} = (\overleftrightarrow{G}_{stot} + \overleftrightarrow{G}_{ptot})\vec{P}_0 = \overleftrightarrow{G}_{tot}\vec{P}_0. \tag{26}$$

The total Poynting vector magnitude (S) is found by squaring and summing the electric field amplitudes for each dipole orientation, according to Eq. (13). For an ensemble of randomly oriented, incoherent dipoles of magnitude P_0, the power from the three possible dipole orientations is averaged. Since an individual dipole could be oriented, e.g., between the x and z axes, it might seem that the x and z components of $\vec{P}_0$ could produce mutually interfering electric fields and that the field should be found for each possible orientation and integrated before solving for S. However, for a random ensemble, the constructive/destructive effect of the dipole x and z components interfering with each other is always matched by a destructive/constructive effect from some complementary dipole with opposite x or z components. Thus, once the planar polarization densities are integrated into δ function densities, then the fields may be squared, and all components and dipole orientations may be summed and divided by 3.[19]

For s-polarized radiation, the result is

$$S_s = |t_{31s}(k_c)|^2\ \frac{c\ k_0^4 n_1^3 \cos^2\theta|\beta_{sc} + 1|^2}{24\ r^2\pi\sigma\ |\mu_{sc}|^2}\ P_0^2, \tag{27}$$

and for p-polarized,

$$S_p = |t_{31p}(k_c)|^2 \frac{c\, k_0^4 n_1 \cos^2\theta(\sigma|\beta_{pc}-1|^2 + n_1^2\sin^2\theta|\beta_{pc}+1|^2)}{24\,\pi\, r^2\sigma\, |n_3|^2|\mu_{pc}|^2} P_0^2, \tag{28}$$

where

$$\sigma = |n_3^2 - n_1^2\sin^2\theta|. \tag{29}$$

To find the power passing through a detector aperture subtending half-angle θ_{obj}, we integrate

$$P(E) = \int_0^{2\pi}\int_0^{\theta_{obj}} (S_s + S_p) r^2 \sin\theta d\theta d\varphi = 2\pi r^2 \int_0^{\theta_{obj}} S_{tot} \sin\theta d\theta, \tag{30}$$

where $P(E)$ is a function of energy because $ck_0 = E/\hbar$, as in Eq. (4).

Let us first examine the homogeneous case, that of a bare dipole outside of any layered structure, where $n_3 = n_1$ and all reflectivity coefficients are zero,

$$P_{bare}(E) = 2\pi \int_0^{\theta_{obj}} \left(\frac{P_o^2 c\, k_0^4 n_1}{12\,\pi\, r^2}\right) r^2 \sin\theta d\theta = P_o^2 c k_0^4 n_1 (1-\cos\theta_{obj})/6. \tag{31}$$

For a randomly oriented radiative recombination event, the ratio P/P_{bare} gives the average fraction of power that radiates into a detector aperture, as a portion of the power which would reach the aperture in the case of no interfaces. That is, given a rate of photons per second which would reach the detector in the homogeneous case, multiplying by P/P_{bare} gives the expected rate of photons per second that would successfully reach the detector in the case of absorption and reflections. If the light-emitting area is sufficiently small, such as that illuminated by a focused laser beam, then the observer position (r, θ) may be considered constant for every part of that area, and P/P_{bare} is the same for all of the region of interest.

For an area $\mathcal{A}$ in the homogeneous case, the LSW formula already tells us the rate R of photons passing through an aperture with solid angle Ω per second, $R = \mathcal{A}\ N(E)\ dE$. Multiplying this by P/P_{bare}, we have the total rate R reaching the detector, which has solid angle $\Omega = 2\pi(1-\cos\theta_{obj})$,

$$R = \int \frac{P(E)\mathcal{A}}{P_{bare}(E)} \frac{a(E)\,(1-\cos\theta_{obj})}{2\pi^2\hbar^3c^2} \frac{E^2}{\exp\left(\frac{(E-\Delta E_F)}{k_B T}\right) - 1}\ dE\,. \tag{32}$$

R is numerically integrated over the energy range of expected luminescence, near the bandgap energy E_g. Note that if ΔE_F becomes large enough to enter the energy range of luminescence, the LSW formula breaks down unless the change in absorption $\alpha(E)$ at high excitation ΔE_F is also accounted for.

If the luminescing portion of a film has a significant thickness, R is also integrated over z_0, with each thin layer dz_0 having an absorptivity of $a(E) = \alpha(E)\, dz_0$, from Eq. (2). Recalling that the values represented by the μ and β symbols remain functions of k_c and hence of θ, the integral over θ in Eq. (30) cannot generally be solved in the closed form, but we will see that a first order approximation in θ is reasonable for typical apertures. We make the common assumption that ΔE_F is flat throughout the absorber, and that any reduction in splitting at the absorber's edge, near the back Ohmic contact, has a negligible effect on total luminescence.[29,30]

III. EXPERIMENTAL DETAILS

To relate the number of photons to a raw detector signal, a standard source of known absolute radiant flux is needed. Small, circular light-emitting diodes (LED) have been suggested,[31] though we found it difficult to keep the LED in the linear output regime while radiating an intensity comparable to an easily measured PL signal. Instead, we used the excitation laser spot on a Spectralon reflectance standard, which has a reflectance of nearly unity with a highly diffuse character. When illuminated with a laser spot of intensity I, the surface of the reflectance standard forms a Lambertian source with radiance I/π. The rate of photons passing through the aperture in this case would be[32]

$$R_{ref} = \mathcal{A}\int_0^{2\pi}\int_0^{\theta_{obj}} \cos\theta \frac{I}{\pi\hbar\omega_L} \sin\theta d\theta d\varphi = \frac{\mathcal{A}I}{\hbar\omega_L}\sin^2\theta_{obj}, \tag{33}$$

where $\hbar\omega_L$ is the photon energy of the laser light. The power $\mathcal{A}I$ can be measured with a power meter, yielding a known R_{ref} for that aperture and laser intensity. A conversion factor C is then found by setting the detector signal (in V or A) equal to CR_{ref}, to account for detector responsivity and any optical losses between the sample surface and the detector. C is also multiplied by the ratio of the detector responsivity at the PL wavelength to the detector responsivity at wavelength 660 nm for the laser. When measuring PL, this allows us to equate the detector signal to CR, obtaining ΔE_F by Eq. (32).

The approach described is validated using solar cells based on CIGS absorbers. The cells were in the substrate configuration, where a 2.5 micron layer of CIGS was deposited on a molybdenum back contact followed by a 70 nm window layer of CdS. The back contact reflectance was taken as 0.3.[33,34] For electrical measurements, devices were completed with a 210 nm ZnO bi-layer and Ni/Al grids. Power conversion efficiencies greater than 15% were obtained when absorbers were graded, with a back contact composition of x = 0.50, a front composition of x = 0.35, and a minimum of x = 0.25, where x = Ga/(Ga + In).[35] Other absorbers were non-graded and fixed at one of two compositions x = 0.50 or 0.35.

For V_{OC} measurements, illumination was provided by a spectrally uniform laser-driven light source filtered from 400 to 850 nm. For PL-I measurement, illumination was provided by a 660 nm diode laser focused by a 6.5× objective lens. $\mathcal{A}$ was found from the spot diameter, or full width at half maximum (FWHM), of 150 μm which was obtained using the standard knife edge method.[36] The power was measured with a NIST-traceable power meter.

The resulting PL was collected through the same objective used to focus the excitation laser, with $\theta_{obj} = 10°$ and aperture NA = 0.17, and passed through filters to remove laser light. The PL intensity was recorded by an InGaAs photodiode connected to a lock-in amplifier. The laser intensity was changed over six orders of magnitude by a series of calibrated neutral density filters.

IV. RESULTS

For photon energies in the range of PL, about 1.1 to 1.3 eV, the complex index of refraction for CIGS at varying alloy composition (x) was used,[10] and the CdS window was assumed to have a real index of refraction of 2.3. Resulting calculations are shown in Fig. 3(a) for x = 0.50, using either a full numerical integration over θ or by approximating the integrand in Eq. (30) to first order in θ, as $f(\theta) \approx f(0) + \theta f'(0)$. For most values of the aperture size θ_{obj}, corresponding to NA $\lesssim$0.5 in air, the first order approximation appears to be adequate. In Fig. 3(b), an example calculation is shown. For convenience as a reference, it is given under the simplified conditions of a $CuIn_{0.5}Ga_{0.5}Se_2$ absorber layer with no CdS coating in air and a back reflectance of unity. The simplified conditions give a 15% larger signal for a fixed ΔE_f. Photons are passing through an objective with θ_{obj} = 10° at room temperature.

The measured PL intensity is equal to CR. Since C is established by the calibration, the value of quasi-Fermi level splitting ΔE_F is found which corresponds to the correct value for R in Eq. (32). This ΔE_F is shown in Fig. 4, where it is compared to the terminal open-circuit voltage V_{OC}, each found at a range of excitation intensities. The ranges generally do not quite overlap, since it is difficult to maintain intensities greater than 10 equivalent suns over a wide area for V_{OC} measurements, while PL is difficult to detect at lower excitation intensities. Even with the same excitation, the terminal V_{OC} is not necessarily the same as ΔE_F, but the departure is often small in CIGS.[29]

The increase in implied ΔE_F as x increases from 0.35 to 0.5 can be seen either with V_{OC} or with optical measurements. For the graded sample, ΔE_F is the largest, and the PL can be

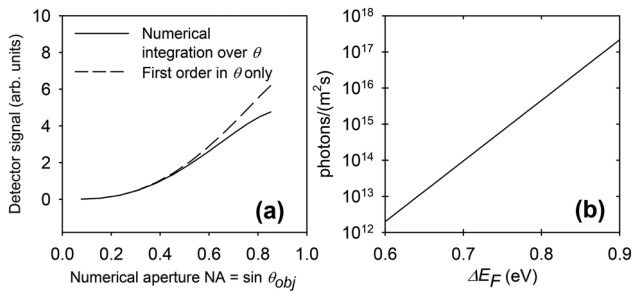

FIG. 3. (a) Calculated detector signal as a function of the aperture opening, comparing full integration over the polar angle with taking only the first order. (b) Example of calculated photons per second entering into objective with aperture NA = 0.17.

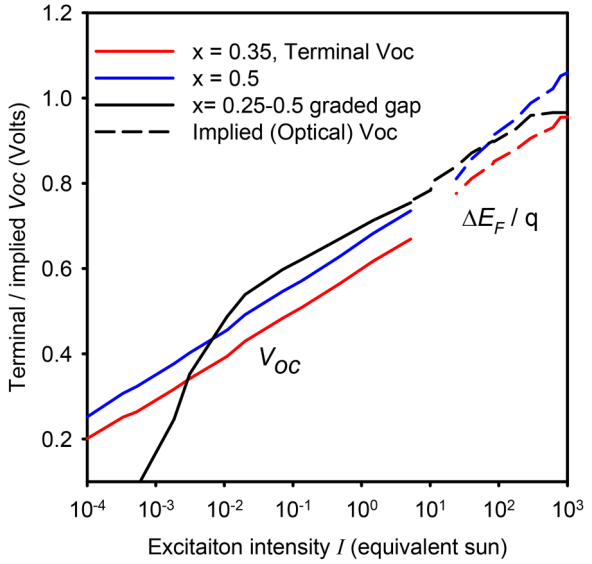

FIG. 4. Comparison of the measured open circuit voltage to the quasi-Fermi level splitting extracted directly from the measured PL intensity without free parameters. An intensity of 1.7×10^{17} photons cm^{-2} s^{-1} is labeled as an equivalent sun.

detected at the lowest I. It appears that at high intensities, ΔE_F for this sample falls below that of the 0.5 sample. This is at least partly due to the majority of the PL coming from a position z_0 near the minimum energy gap within the graded material. This allows the relatively high ΔE_F to quickly reach a level where it would overlap the relatively low energy of the emitted PL spectrum at the bandgap minimum. This means that the use of a fixed α(E) in the LSW formula breaks down for the highest excitations I in the graded gap absorber, where the excitation is strong enough to change α(E) from its literature value.[10]

V. CONCLUSIONS

The luminescence from a source within a slab of known optical constants is found for the first time in a way which includes re-absorption and interference with front and back interfaces. This leads immediately to a quantitative relationship between ΔE_F and radiance. Using a radiance standard, an absolute relationship between the detector signal and ΔE_F can also be obtained. The calculation contains a double numerical integration over energy and depth, but a triple integration to include the polar coordinate should not be necessary. No calibration cells with independently known ΔE_F values are needed, nor are any assumptions concerning band offsets or electrical properties, so long as the optical properties are known and ΔE_F is approximately flat through most of the absorber region. The PL method is useful for as-grown material stacks and does not require additional device processing. Furthermore, it is applicable to other photonic devices such as

light-emitting diodes where the evaluation of the quasi-Fermi level splitting is important.

ACKNOWLEDGMENTS

This work was supported by the U.S. Department of Energy's (DOE) Office of Energy Efficiency and Renewable Energy (EERE) under Solar Energy Technologies Office (SETO) Agreement No. DE-EE0007541. This work was authored in part by the National Renewable Energy Laboratory, operated by the Alliance for Sustainable Energy, LLC, for the U.S. Department of Energy (DOE) under Contract No. DE-AC36-08GO28308. The views expressed in the article do not necessarily represent the views of the DOE or the U.S. Government. The U.S. Government retains and the publisher, by accepting the article for publication, acknowledges that the U.S. Government retains a nonexclusive, paid-up, irrevocable, worldwide license to publish or reproduce the published form of this work, or allow others to do so, for U.S. Government purposes.

REFERENCES

[1]T. Trupke, B. Mitchell, J. W. Weber, W. McMillan, R. A. Bardos, and R. Kroeze, Energy Procedia **15**, 135 (2012).
[2]H. Höffler, H. Al-Mohtaseb, J. Haunschild, B. Michl, and M. Kasemann, J. Appl. Phys. **115**, 034508 (2014).
[3]B. Hallam, B. Tjahjono, T. Trupke, and S. Wenham, J. Appl. Phys. **115**, 044901 (2014).
[4]O. Breitenstein, H. Höffler, and J. Haunschild, Sol. Energy Mater. Sol. Cells **128**, 296 (2014).
[5]G. J. M. Janssen, Y. Wu, K. C. J. J. Tool, I. G. Romijn, and A. Fell, Energy Procedia **92**, 88 (2016).
[6]G. Rey, C. Spindler, F. Babbe, W. Rachad, S. Siebentritt, M. Nuys, R. Carius, S. Li, and C. Platzer-Björkman, Phys. Rev. Appl. **9**, 064008 (2018).
[7]A. Redinger, S. Kretzschmar, and T. Unold, in *2016 IEEE 43rd Photovoltaic Specialists Conference (PVSC), Portland, OR, 5–10 June 2016* (IEEE, 2016), p. 3559.
[8]J. K. Katahara and H. W. Hillhouse, J. Appl. Phys. **116**, 173504 (2014).
[9]P. Wurfel, *Physics of Solar Cells: From Principles to New Concepts* (Wiley-VCH, Weinheim, Germany, 2005), pp. 66–67.
[10]P. Aryal, A.-R. Ibdah, P. Pradhan, D. Attygalle, P. Koirala, N. J. Podraza, S. Marsillac, R. W. Collins, and J. Li, Prog. Photovoltaics Res. Appl. **24**, 1200 (2016).
[11]O. D. Miller, E. Yablonovitch, and S. R. Kurtz, IEEE J. Photovolt. **2**, 303 (2012).
[12]U. Rau, Phys. Rev. B **76**, 085303 (2007).
[13]T. Trupke, E. Daub, and P. Würfel, Sol. Energy Mater. Sol. Cells **53**, 103 (1998).
[14]S. M. Durbin, J. L. Gray, R. K. Ahrenkiel, and D. H. Levi, in *23rd IEEE Photovoltaic Specialists Conference, Louisville, KY, 10–14 May 1993* (IEEE, Danvers, MA, 1993), p. 628.
[15]M. A. Steiner, J. F. Geisz, I. García, D. J. Friedman, A. Duda, and S. R. Kurtz, J. Appl. Phys. **113**, 123109 (2013).
[16]A. Niv, M. Gharghi, C. Gladden, O. D. Miller, and X. Zhang, Phys. Rev. Lett. **109**, 138701 (2012).
[17]L. D. Landau and E. M. Lifshitz, in *Statistical Physics*, 3rd ed., edited by L. D. Landau and E. M. Lifshitz (Butterworth-Heinemann, Oxford, 1980), p. 333.
[18]J. K. Larsen, S. Y. Li, J. J. S. Scragg, Y. Ren, C. Hägglund, M. D. Heinemann, S. Kretzschmar, T. Unold, and C. Platzer-Björkman, J. Appl. Phys. **118**, 035307 (2015).
[19]W. Lukosz, J. Opt. Soc. Am. **71**, 744 (1981).
[20]R. T. Holm, S. W. McKnight, E. D. Palik, and W. Lukosz, Appl. Opt. **21**, 2512 (1982).
[21]S. R. J. Brueck, V. A. Smagley, and P. G. Eliseev, Phys. Rev. E **68**, 036608 (2003).
[22]E. H. Hellen and D. Axelrod, J. Opt. Soc. Am. B **4**, 337 (1987).
[23]H. F. Arnoldus and J. T. Foley, J. Opt. Soc. Am. A **21**, 1109 (2004).
[24]M. G. Abebe, A. Abass, G. Gomard, L. Zschiedrich, U. Lemmer, B. S. Richards, C. Rockstuhl, and U. W. Paetzold, Phys. Rev. B **98**, 075141 (2018).
[25]M. Paulus, P. Gay-Balmaz, and O. J. F. Martin, Phys. Rev. E **62**, 5797 (2000).
[26]J. E. Sipe, J. Opt. Soc. Am. B **4**, 481 (1987).
[27]M. C. Troparevsky, A. S. Sabau, A. R. Lupini, and Z. Zhang, Opt. Express **18**, 24715 (2010).
[28]G. B. Arfken, H. J. Weber, and F. E. Harris, *Mathematical Methods for Physicists* (Elsevier Inc., Waltham, MA, 2012), pp. 585–590.
[29]G. H. Bauer, R. Brüggemann, S. Tardon, S. Vignoli, and R. Kniese, Thin Solid Films **480–481**, 410 (2005).
[30]R. Brüggemann, P. Schulze, O. Neumann, W. Witte, and G. H. Bauer, Thin Solid Films **535**, 283 (2013).
[31]M. Yoshita, H. Kubota, M. Shimogawara, K. Mori, Y. Ohmiya, and H. Akiyama, Rev. Sci. Instrum. **88**, 093704 (2017).
[32]R. McCluney, *Introduction to Radiometry and Photometry* (Artech House, Boston, 2014), p. 13.
[33]J. Malmström, S. Schleussner, and L. Stolt, Appl. Phys. Lett. **85**, 2634 (2004).
[34]N. Dahan, Z. Jehl, T. Hildebrandt, J. J. Greffet, J. F. Guillemoles, D. Lincot, and N. Naghavi, J. Appl. Phys. **112**, 094902 (2012).
[35]I. Repins, L. Mansfield, A. Kanevce, S. A. Jensen, D. Kuciauskas, S. Glynn, T. Barnes, W. Metzger, J. Burst, C. S. Jiang, P. Dippo, S. Harvey, G. Teeter, C. Perkins, B. Egaas, A. Zakutayev, J. H. Alsmeier, T. Lußky, L. Korte, R. G. Wilks, M. Bär, Y. Yan, S. Lany, P. Zawadzki, J. S. Park, and S. Wei, in *2016 IEEE 43rd Photovoltaic Specialists Conference (PVSC), 5–10 June 2016* (IEEE, Danvers, MA, 2016), p. 0309.
[36]M. Passlack, R. N. Legge, D. Convey, Z. Y. Yu, and J. K. Abrokwah, IEEE Trans. Instrum. Meas. **47**, 1362 (1998).